Journal of Materials Chemistry A

Accepted Manuscript

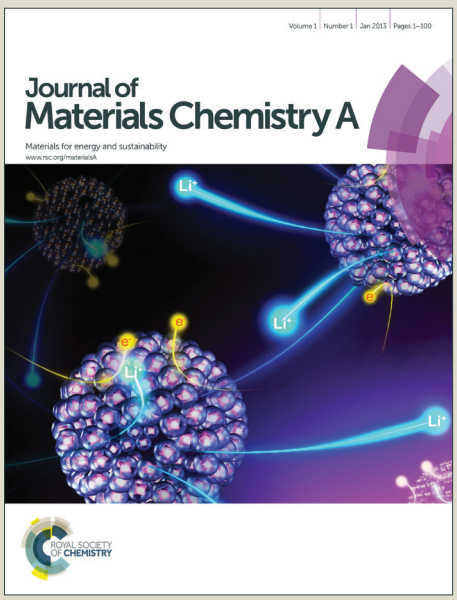

ROYAL SOCIETY OF CHEMISTRY

www.rsc.org/materialsA

Journal Name

RSCPublishing

ARTICLE

Highly Selective Carbon Dioxide Adsorption on Exposed Magnesium Metals in A Cross-Linked Organo-Magnesium Complex

Cite this: DOI: 10.1039/x0xx00000x

Received 00th January 2012,
Accepted 00th January 2012

DOI: 10.1039/x0xx00000x

www.rsc.org/

Kapil Pareek,[a] Qingfan Zhang,[a,b] Rupesh Rohan[a] and Hansong Cheng[a,b] ,

A cross-linked organo-magnesium complex (MTF-Mg) was synthesized and investigated for selective CO_2 adsorption over N_2 at 298K. Remarkably high selectivity and reversibility were achieved with an isosteric heat of adsorption of 45.2 kJ/mol for CO_2, consistent with the predicted DFT value of 37.3 kJ/mol. The CO_2 preferential adsorption arises from its strong interaction with the exposed magnesium atoms.

Introduction

The sharply rising level of carbon dioxide emission from combustion of fossil fuels has raised increasing environmental concerns on global warming and climate change. Approximately 40-50 % of total CO_2 emission comes from stationary sources, such as power plants and steel mills.[1] Storage materials with high capacity and high selectivity for CO_2 capture are in increasing demand. In general, CO_2 capture and separation from power plants can be done in three stages, termed as pre-combustion, post-combustion and oxy-combustion.[2] Selective CO_2/N_2 separation from flue gas is required for the post-combustion stage.[3] In a typical post-combustion flue gas composition, selective separation of CO_2/N_2 presents a formidable technical challenge due to a relatively low concentration of CO_2 (15-16%) and a large quantity of N_2 (73-77%).[4] Therefore, development of highly selective adsorbents towards CO_2 over N_2 is crucial for CO_2 capture and subsequent sequestration.

Current technologies for post-combustion CO_2 capture are largely based on the process of passing flue gas through an aqueous amine-based solution with high selectivity, fast kinetics but a moderate capacity for CO_2 absorption at a near ambient temperature.[2] CO_2 molecules form covalent bonds with the amino groups of the absorbent to produce carbamate species and are subsequently released for sequestration or utilization at a temperature typically above 100 ^oC.[5] The solution based absorption technology usually causes ca. 30 % energy penalty during the regeneration process.[6] In particular, the high water content in the solution, required for reducing the viscosity and enhancing the absorption kinetics, makes the process even more expensive due to the large heat capacity of water, which does not directly contribute to CO_2 uptake and removal. Furthermore, thermal and oxidative degradation of solvents may also take place in the absorbent recovery process at an elevated temperature, which produces undesirable corrosive by-products.[2]

Pressure swing adsorption (PSA) technology has long been widely practiced for industrial scale gas separation with a high efficiency.[1] For a gas mixture, the effectiveness of the PSA technology is largely dependent on the selectivity and capacity of the adsorbent toward an individual gas molecule of interest. Selective CO_2 adsorption from flue gas has been extensively investigated with a wide variety of porous materials, such as metal organic framework (MOF) compounds,[3, 7] activated carbons,[8] zeolites,[9] and covalent-organic frameworks (COFs) at near ambient conditions.[1, 3,10] However, the low hydrothermal stability[11, 12] and relatively slow adsorption kinetics[13] of these materials limit the broad applicability of the adsorption technology for pre- or post-combustion CO_2 capture. Amorphous porous covalent organic materials,[10] which possess large surface areas and a tunable pore size, show higher hydrothermal stability than MOFs and COFs.[11, 14] A series of covalent organic materials, along with conjugated microporous polymers and covalent organic polymers, have been investigated in recent years for selective CO_2 capture from flue gas under ambient conditions.[15-17] Remarkably, introduction of CO_2-philic moieties or polar functionalities into these materials was found to exert profound influence on both CO_2/N_2 selectivity and heat of CO_2 adsorption. Furthermore, the role of the polar groups (e.g. –OH and $–NH_2$)[16, 18, 19] and monovalent cations (e.g. Li^+ and Na^+)[14] incorporated in the adsorbents via pre or post-synthesis modifications in enhancing CO_2 capture

selectivity and capacity, has been extensively investigated and proven to be reasonably effective.[1] These ionic species are well-coordinated in the polymer matrix, which however compromises the interaction with CO_2 and thus leads to a relatively low enthalpy of adsorption. Unfortunately, to date, little attempt has been made to incorporate multivalent cations in porous organic network environment for selective CO_2 adsorption.[1] It is anticipated that introduction of under-coordinated multivalent cations in these materials may radically enhance the adsorption selectivity as well as capacity.

In this article, we report successful synthesis of an organo-magnesium functionalized cross-linked melamine-terephthaldehyde framework (MTF-Mg) for selective CO_2 adsorption over N_2 at 298K. The compound was prepared by reacting Mg-modified-melamine with terephthaldehyde. Melamine-terephthaldehyde based cross-linked organic framework complexes without metal incorporation have been recently reported to be quite porous with a surface area ranging from 300 m^2/g to 1377 m^2/g.[20, 21] However, these materials were found to indiscriminately adsorb the molecular species in the flue gas with poor CO_2 selectivity over N_2. (Fig. S1 Supporting Information) By adopting a similar synthetic protocol but incorporating organo-magnesium moiety in the precursors, we obtained a material with a moderate surface area and exposed magnesium metal sites. The synthesized MTF-Mg complex exhibits remarkably high CO_2/N_2 selectivity of 32 at 298K and 1 atm, comparable to the selectivity found in several MOF materials deemed to be excellent candidates for post combustion CO_2 capture as adsorbents under similar conditions.[1] The selectivity of the MTF-Mg complex is also comparable to the value of the post-modified metal functionalized porous aromatic framework materials with moderate surface areas (430-717 m^2/g).[22] The significantly higher selectivity than the value of previously reported melamine-terephthaldehyde based framework compounds[23] is largely attributed to the high exposure of magnesium cations on the walls of the porous compound to the gas molecules. The novel approach of incorporating multivalent cations in the high porous organic framework might lead to design of new materials with under-coordinated metals for selective CO_2 adsorption from flue gas via PSA technology.

Experimental

Synthesis of MTF-Mg copolymer

The MTF-Mg copolymer was synthesized in a two-step reaction, as shown schematically in Scheme 1. In the first step, a flame-dried three neck flask fitted with a condenser and a magnetic stirring bar was charged with melamine (500 mg, 3.96 mmol) and a hexane (40 ml) solvent under argon atmosphere at -78 °C. Subsequently, di-butyl magnesium (5.94 mmol) was injected to the flask and stirred for 12 hrs under argon atmosphere, producing the Mg-modified-melamine complex and butane gas. In the second step, 1,4-benzenedicarboxaldehyde (796 mg, 5.94 mmol) and diglyme (40 ml) were added into the reaction mixture, which was then stirred at 160 °C for 72 hrs under argon atmosphere. Upon cooling to room temperature, the precipitated MTF-Mg was filtered and washed with an excess of anhydrous acetone, anhydrous tetrahydrofuran, and anhydrous dichloromethane, respectively. The solvents were removed under a reduced pressure by using a rotary evaporator. Final drying was done at 190 °C under vacuum in a tube furnace to produce a yellow powder with a yield of 70 %.

FTIR (MTF-Mg): ῡ (triazine ring) 1550 cm^{-1}, 1480 cm^{-1}, ῡ (adsorbed moisture) 3200-3400 cm^{-1} (b)

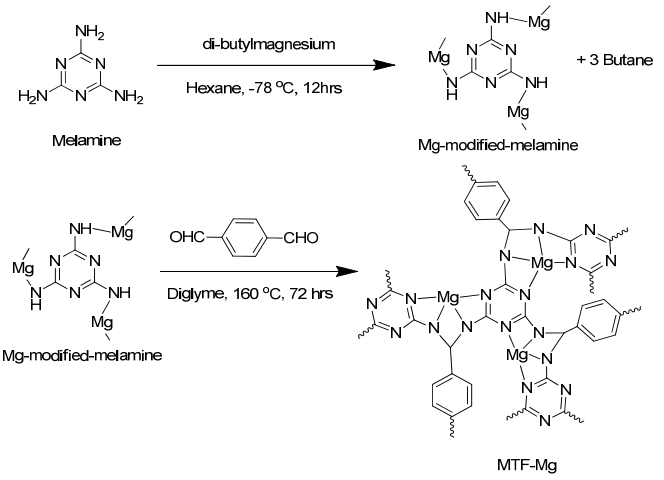

Scheme 1. The synthetic protocol of the MTF-Mg complex.

Characterization

The nitrogen adsorption-desorption isotherms at 77K and 1 atm were measured on ASAP 2020. The Brunauer-Emmett-Teller (BET) surface area was calculated over the range of relative pressure of 0.05-0.20 bar. The sample was activated at 120 °C under vacuum for 12 h prior to the measurement.

Powder X-ray diffraction (XRD) was performed on a D5005 Bruker AXS diffractometer with Cu-Kα radiation (λ = 1.5410) at room temperature. The diffraction pattern of the MTF-Mg was measured using a sample size of 70-110 mg. SEM images were obtained using a scanning electron microscopy (SEM) with Jeol JSM-6701F. Samples were prepared by gold sputtering under 9Pa at room temperature (20s, 30mA) with a JEOL JFC 1600 Fine Coater. All X-ray photoelectron spectra (XPS) were taken with a VG Scientific ESCALAB MKII spectrometer. Infrared spectroscopy was taken on the Varian resolutions (version 4.0.5.009). Thermogravimetric analysis was performed on a TA instrument 2960 (DTA-TGA) from room temperature to 900 °C at the heating rate of 5 °C/ min.

Gas adsorption isotherms were obtained by using a computer-controlled commercial Gas Reaction Controller (GRC) manufactured by Advanced Materials Corporation. The GRC instrument is based on a volumetric method to determine gas

adsorption and was calibrated by following the standard practice guidelines recommended by US DOE.[24] The empty sample chamber was tested to determine its zero adsorption baseline at 298K and 77K, respectively (Fig. S5, Supporting Information). Furthermore, the GRC was also calibrated with commercially available standard materials basolite A100 (MIL53-Al MOF) and $LaNi_5$ alloy at 77K and 298K, respectively (Figs. S6 and S7, Supporting Information). High purity CO_2 (99.8) and N_2 (99.995) gases were used for the adsorption measurements.

All gas adsorption-desorption measurements were performed following the standard procedure.[25-27] Around 300 mg of MTF-Mg was sealed in a sample chamber inside the glove box to prevent exposure to the moisture and was subsequently activated at 150 ^{0}C under a reduced pressure (below 10^{-5} torr) for overnight on the GRC. The adsorption-desorption isotherms of the MTF-Mg complex were measured at 273K and 298K over a pressure range of 0-1 atm.

The skeleton density of the compound was measured using a Quantachrome Ultrapyc 1200e instrument, which was calibrated using a sphere with a known volume. The skeleton density of the MTF-Mg complex (1.6 g/cc) was provided to the GRC to obtain an accurate void space volume by subtracting the skeleton volume of the sample from the volume of the sample chamber.

Enthalpies of adsorption were derived from the following equation.[28]

$$\left[\frac{\partial \ln p}{\partial \left(\frac{1}{T}\right)}\right]_\theta = -\frac{\Delta_{ad}H}{R} \quad , \qquad (1)$$

where T represents the temperature, p is the pressure (in kPa), $\Delta_{ad}H$ is the enthalpy of adsorption and R is the universal gas constant. [28] A plot of ln$p$ against 1/T is a straight line of the slope $\Delta_{ad}H/R$ at a given surface coverage.

The selectivity of CO_2 of the MTF-Mg sample was evaluated using the experimental single-component gas adsorption isotherms based on the following equation: [1, 13]

$$S = \frac{q_1 / q_2}{p_1 / p_2} \quad , \qquad (2)$$

where S is the selectivity factor, q_1 and q_2 represent the adsorbed quantities of components 1 and 2, and p_1 and p_2 stand for the partial pressures of components 1 and 2, respectively. For post-combustion flue gas, the partial pressures of CO_2 and N_2 are 0.15 bar and 0.75 bar, respectively.[1]

Computational method

To assist elucidation of the experimental results, first principles calculations based on density functional theory (DFT) were carried out under the generalized gradient approximation (GGA) using the Perdew-Burke-Ernzerhof (PBE) exchange correlation functional as implemented in the DMOl^3 code.[29] A double numerical basis set augmented with polarization functions was employed to describe the valence electrons with the core electrons represented by an effective core potential. The interaction between CO_2 and the host was calculated upon full geometry optimization using a local structural model in the proximity of the Mg atom of the MTF-Mg complex shown in Scheme 1. Subsequently, the adsorption energy was evaluated using the following equation:

$$E_{ads} = E_{MTF\text{-}Mg+CO2} - E_{MTF\text{-}Mg} - E_{CO2} \,, \qquad (3)$$

where $E_{MTF\text{-}Mg+CO2}$, $E_{MTF\text{-}Mg,}$ and E_{CO2} represent the energies of the MTF-Mg complex with an adsorbed CO_2 molecule, the energy of the MTF-Mg complex and the energy of the CO_2 molecule, respectively.

Results and discussions

Table 1. Elemental analysis results of the MTF-Mg complex.

Compound		C%	H%	N%	Mg%
MTF-Mg	Expected	45.94	2.97	35.74	15.50
	Found	35.95	3.89	28.54	12.84

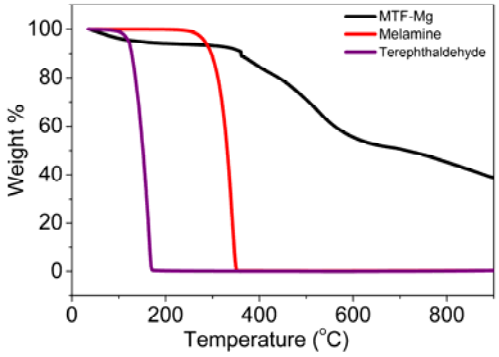

Figure 1. TGA thermograms of melamine (red), terephthaldehyde (purple), and MTF-Mg (black) under nitrogen atmosphere at 5 °C/min heating rate.

The first evidence of successful synthesis of the designed MTF-Mg complex is provided by the elemental analysis, which yields a reasonable match between the expected and the detected data (Table 1). The TGA thermograms of the starting materials and the synthesized MTF-Mg compound are displayed in Fig. 1. The MTF-Mg complex shows a steep weight loss at ca. 468 °C, which is higher than the degradation temperatures of both melamine and terephthaldehyde, clearly supporting the expected polymerization reaction between the Mg-modified-melamine precursor and terephthaldehyde. In addition, the MTF-Mg complex displays a higher char residue of 40% at 900 °C than the previously reported melamine-terephthaldehyde framework[20, 21, 30] due to the presence of the organo-magnesium moiety.

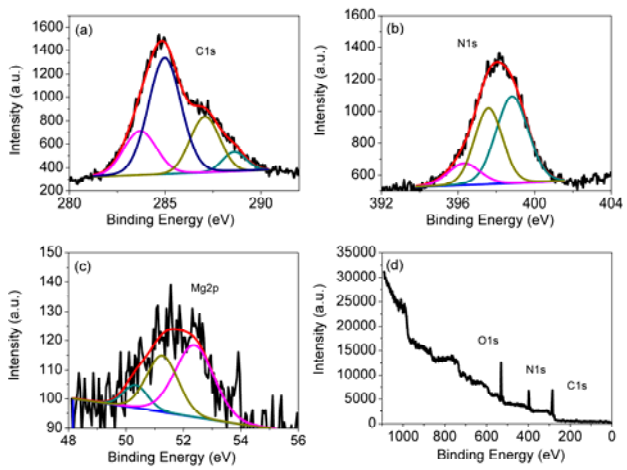

Figure 2. X-ray photoelectron spectra of the MTF-Mg copolymer (a) high resolution scan of C1s, (b) high resolution scan of N1s, (c) high resolution scan of Mg2p, and (d) a complete scan.

The X-ray photoelectron spectra (XPS) of the MTF-Mg complex are shown in Fig. 2. The C1s core level shift of the material (Fig. 2a) can be fitted into four peaks, corresponding to the carbon atoms in the benzene ring (283.63 eV), the linkers (the carbon atom bonded to the more electronegative N or O atoms 284.98, 287.10 eV) and the triazine ring (288.60 eV), respectively.[31, 32] The peak for the O1s band is due to the C-OH group formed during the condensation reaction and some un-reacted C=O groups of the terephthaldehyde monomer.[20] The N1s band can be fitted into three peaks at 396.31, 397.56 and 398.81 eV. The peak at 396.31 eV corresponds to the nitrogen atoms of the triazine ring (C=N-C) and the remaining two peaks at 397.56 and 398.81 eV are associated with the nitrogen atoms of the amine groups coordinated to the magnesium metals.[20] The energy band of Mg 2p can be approximately fitted into a group of three peaks located at 50.33, (Mg bonded with O containing groups) 51.26 (Mg-N) and 52.38 eV, (Mg-N) respectively (Fig. 2c), reflecting different chemical environments. The high binding energy of the Mg 2p peaks is attributed to the high electronegativity of the nitrogen atoms and the charge delocalization into the aromatic ring derived from the N-Mg bonds.

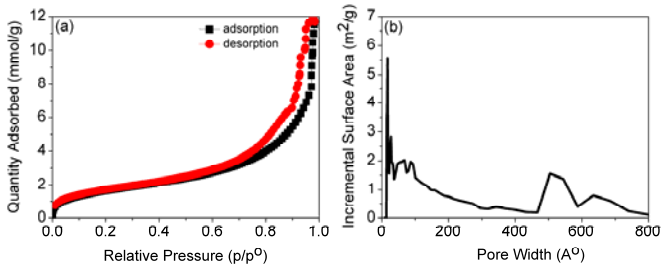

Figure 3. (a) Nitrogen adsorption-desorption isotherms at 77K for MTF-Mg, (b) pore size distribution calculated from the nitrogen isotherm at 77K by applying the DFT pore size analysis method.

The specific surface area of the MTF-Mg complex was measured at 77K by nitrogen adsorption-desorption isotherms (Fig 3a). The compound displays a BET surface area of 137 m^2/g and a Langmuir surface area of 222 m^2/g, respectively. The surface area of MTF-Mg is significantly lower than the reported values of the melamine-terephthaldehyde based network compounds without metal incorporation (300-1377 m^2/g), [20, 33, 34] most of MOF materials (150-5000 m^2/g)[28] and porous carbons (100-1500 m^2/g).[35] The relatively low surface area of the MTF-Mg complex is attributed to the functionalization of the organo-magnesium moiety into the polymer network with the exposed magnesium atoms pulling nearby nitrogen atoms toward the cationic sites, which effectively facilitates pore size shrinkage. Indeed, the DFT pore size distribution (PSD) of the MTF-Mg complex (Fig. 3b) clearly indicates the presence of a wide range of nano-pores, which differs significantly from the narrow PSD observed for melamine-terephthaldehyde based network compounds without metal incorporation.[20, 21] In addition, the total calculated volume of the pores is up to 0.40 cm^3/g, which is comparable to the reported data without metals.[20, 21] The change in PSD without changing the total pore volume in MTF-Mg may arise from the different framework topology of the material upon metal functionalization.

The porous structure of the MTF-Mg complex was further investigated by scanning electron microscopy (SEM). The SEM image shown in Fig. 4 reveals that the agglomerates are interconnected with each other to form a continuous porous network. These amorphous, loosely packed structures are important for enhancing the accessibility of gas molecules to the active sites of the material.[20]

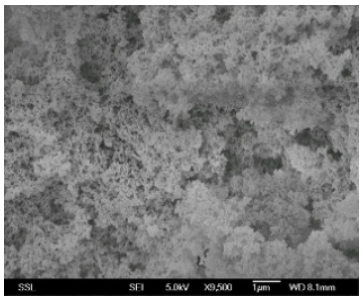

Figure 4. SEM micrograph of MTF-Mg copolymer.

The adsorption isotherms of CO_2 and N_2 at 298K and up to 1 atm pressure are shown in Fig. 5a. Remarkably, the uptake of CO_2 rises sharply as the pressure increases, while the adsorption capacity of N_2 remains essentially flat in the pressure range. The results indicate that the host material interacts with the CO_2 molecules more strongly than with N_2. The compound displays a room temperature CO_2 capacity of 1.96 wt% at 1 atm pressure without saturation with high adsorption reversibility. The maximum error in the measurement is up to 0.07 wt%. The sorption of CO_2 was found to be completely reversible at 298K

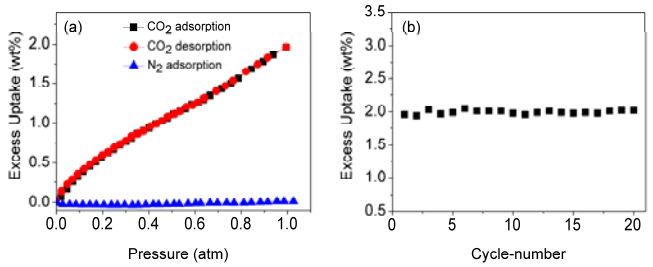

Figure 5. (a) Adsorption isotherms of CO_2 and N_2 on MTF-Mg at 298K and 1 atm pressure and (b) CO_2 excess capacity at 298K in twenty one fully reversible adsorption-desorption cycles up to 1 atm pressure.

and 1 atm with the cycle performance demonstrated in Fig. 5b. The selective adsorption of CO_2 over N_2 estimated from the single-component isotherms[1] reveals that the MTF-Mg copolymer shows CO_2/N_2 selectivity of 32 at 298K and 1 atm pressure. The CO_2/N_2 selectivity of the MTF-Mg complex is comparable to the reported selectivity found in several high surface area MOF materials, which have been regarded as highly promising adsorbents for post combustion CO2 capture under similar experimental conditions. These compounds include Mg_2(dobdc) (CO_2/N_2= 44 at 303K; SSA 1174 m^2/g),[36] CuTATB-60 (CO_2/N_2= 24 at 298K; SSA 3811 m^2/g),[37] Fe-BTT (CO_2/N_2= 18 at 298K; SSA 2010 m^2/g),[38] ZIF-78 (CO_2/N_2= 30 at 298K; SSA 620 m^2/g),[39] Cu-BTT-ri (CO_2/N_2= 19 at 298K; SSA 1770 m^2/g),[18] and ZIF-100 (CO_2/N_2= 22 at 298K; SSA 595 m^2/g).[40] The selectivity is also comparable to the reported values of post-modified monovalent metal functionalized porous aromatic frameworks (PAF-26-COOLi, SSA 591 m^2/g CO_2/N_2= 24; PAF-26-COONa, SSA 483 m^2/g CO_2/N_2= 53; PAF-26-COOK, SSA 4301 m^2/g CO_2/N_2= 50).[22]

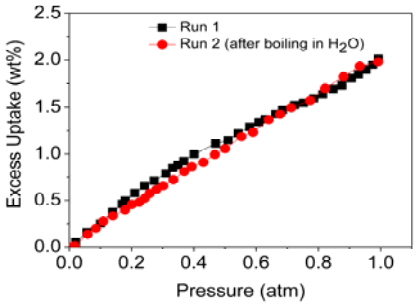

Figure 6. Excess CO_2 adsorption capacity for MTF-Mg at 298K and 1 atm (Run 1). Run 2 employed material regenerated after run 1 by boiling in water for 1h.

CO_2 capture from flue gas requires adsorbents to be hydrothermally stable as post combustion flue gas contains ca. 5-7% (by volume) of water. Figure 6 depicts two adsorption isotherms measured for MTF-Mg with and without water treatment. The water treatment was done by immersing the compound in boiled water for an hour.[14] The results shown in Fig. 6 demonstrate that there is no obvious loss in CO_2 uptake capacity and confirm the ultrahigh stability of the material for practical applications. Nevertheless, the presence of water vapour in post combustion flue gas may show a negative effect on CO_2 adsorption by reducing its uptake as reported by Gang Li et al.[41]

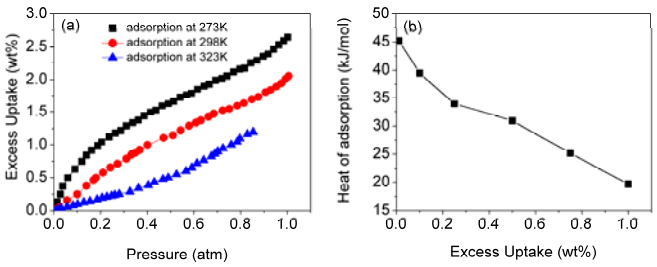

Figure 7. (a) Excess carbon dioxide uptake at 323K, 298K and 273K, and (b) calculated isostearic heat of adsorption of CO_2 on MTF-Mg.

To quantitatively describe the adsorption strength, the isostearic heat of adsorption was derived from the measured isotherms at 323K, 298K and 273K using the equation (1) (Fig.7). The low coverage isosteric heat of adsorption calculated from isotherms at 323K, 298K and 273K was found to be up to 45.2 kJ/mol.

The low coverage isosteric heat of CO_2 adsorption of MTF-Mg is higher than the reported values for melamine-terephthaldehyde frameworks (31.5 kJ/mol), post metal modified porous aromatic frameworks (28.1-35.0 kJ/mol),[22] SO_3H (30.4 kJ/mol) and SO_3Li (35.7 kJ/mol) grafted porous polymer network,[14] comparable to many highly CO_2 selective MOF materials, such as CuTATB-30 (48 kJ/mol),[37] Mg-MOF-74 (47 kJ/mol),[42] and significantly lower than the value in Cu-BTTri-en (90 kJ/mol).[18] The isosteric heat of adsorption decreases monotonically with the surface coverage. We note here that it is possible that adsorption can also be limited by gas diffusion in the polymer matrix rather than kinetics. For MTF-Mg, it is estimated that the desorption energy of 45.2 kJ/mol would allow CO_2 release with a partial pressure of 0.005bar at 282K, while for a desorption energy of 90 kJ/mol, the temperature would have to be raised to 500K to achieve the same partial pressure (Supporting Information).

The high selectivity and adequate heat of adsorption observed in the MTF-Mg complex are attributed to the relatively more exposed divalent cations than the active metal sites in many coordinatively unsaturated MOF materials, in which the metal sites become essentially five coordinated upon removal of a metal bonded solvent molecule in the activation process.[43-45] In comparison, each Mg atom in the MTF-Mg complex is chelated by 4 neighbouring N atoms. As revealed by the DFT-optimized local structure with one unit of the MTF-Mg complex based on the hypothetical structure shown in Scheme 1 (Fig. 8a and Table 2), the two slightly shorter N-Mg bonds are formed through the strong covalent interaction between Mg and the neighboring amino groups of the adjacent melamine molecules. Another two slightly longer N-Mg bonds arise from the weak back donation from the nearby N atoms in the two triazine rings. Aside from the low coordination number, the rigid ligand environment provided by the cross-linked polymer network

makes the metal atom even more poorly coordinated as shown in Fig. 8. As a consequence, the metal sites become highly active toward gas molecules. Furthermore, the quadruple moment of CO_2 (13.4 x 10^{-40} Cm^2) is significantly higher than that of N_2 (4.7 x 10^{-40} Cm^2), making the metal sites fully occupied by CO_2 through a strong quadruple-cation interaction.[46] The high CO_2 over N_2 selectivity not only reflects the fact that the metal sites are fully populated by CO_2 but also indicates that it is the metal sites, not the van der Waals forces, that give rise to the strong CO_2 adsorption.

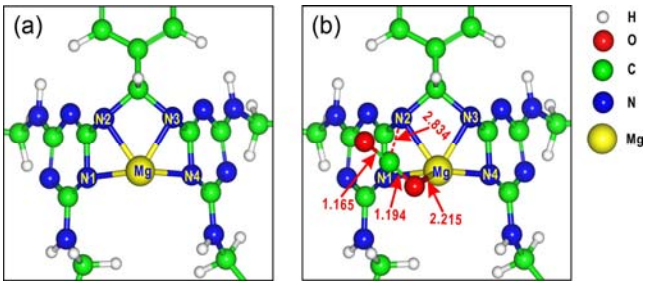

Figure 8. Electrostatic potential surface of the MTF-Mg complex before and after CO_2 adsorption.

To gain atomistic insight into the interaction strength between CO_2 and the host, we performed density functional theory calculations using a model system of one unit of the MTF-Mg complex based on the hypothetical structure shown in Scheme 1 with the neighbouring units terminated with benzene (Fig. 8). This structural arrangement is not expected to give rise to significant uncertainty to the bonding properties in the proximity of the exposed metal site since the termination is done at the distances sufficiently far from the active adsorption site.

Table 2. N-Mg bond distance and Mulliken charge before and after CO_2 adsorption on the MTF-Mg complex.

	N-Mg bond length (A°)		Mulliken Charge (e^-)	
	Before	After	Before	After
N1	2.110	2.130	-0.655	-0.662
N2	2.062	2.107	-0.587	-0.638
N3	2.057	2.063	-0.587	-0.588
N4	2.120	2.129	-0.640	-0.640
Mg	-------	------	0.905	0.946

Figure 8 displays the optimized substrate and adsorption structures. The Mg atom is coordinated by 4 neighbouring N atoms asymmetrically. Upon sampling several possible adsorption configurations, we found that the "side-on" mode of the CO_2 molecule is energetically preferred. One O atom is directly attached to the Mg atom with a short distance of 2.215Å and the positively charged C atom of CO_2 interacts with the most negatively charged N atom near the metal site, forming a 4-membered physisorption structure. Only a slight variation of the C-O bonds relative to the gas-phase value (1.194 Å and 1.165 Å vs. 1.192 Å) was observed. The calculated adsorption energy is 37.3 kJ/mol, in reasonable agreement with the experimentally measured value. The adsorption is dictated chiefly by the bonding interaction between the electron-rich oxygen and the under-coordinated, positively charged Mg atom and, to a less extent, by the electrostatic interaction between the C atom and the amino group in the proximity of the metal site.

Conclusions

Achieving high capacity and high selectivity for CO_2 capture from post-combustion flue gas is important for effective control of greenhouse gas emission. PSA based technologies are ideally well-suited for the purpose with substantially lower costs, relative to the conventional liquid amine-based technologies with temperature control, and operational convenience, if adequate adsorbents that meet specific industrial requirements could be developed. In the present study, we presented a novel approach for synthesis of porous organic framework compounds with highly exposed multivalent metals, which serve as the CO_2 adsorption sites. A magnesium metal functionalized MTF-Mg complex was synthesized via pre-modification of precursors and subsequently characterized. Our results suggest that this material is highly cross-linked with moderate porosity and high thermal stability. The measured BET surface area of 137 m^2/g is significantly smaller than that of the polymeric compound without metal incorporation.

The performance of the MTF-Mg complex toward selective adsorption of CO_2 over N_2 was tested via volumetric adsorption isotherm measurements. Unlike melamine-terephthaldehyde based cross-linked organic framework compounds without metal incorporation, the MTF-Mg complex displays remarkably high CO_2/N_2 selectivity, arising from the larger quadruple moment of CO_2, and an adequate isosteric heat of adsorption, making the compound highly promising for the gas separation. The CO_2 adsorption is also completely reversible and hence, well suited for use of PSA technology.

Despite the high adsorption selectivity and reversibility, the relatively low specific surface area of the complex presents a considerable limit to the adsorption capacity. New synthetic routes need to be explored to develop porous organic framework compounds with higher surface areas but with exposed multivalent metal sites. The results presented in the present study may shed a light on the future development of materials for post-combustion CO_2 capture with high capacity, high selectivity, high reversibility and low cost via PSA technology.

Acknowledgements

The authors gratefully acknowledge support of a Start-up grant from NUS, a POC grant from National Research Foundation of Singapore, a Tier 1 grant from Singapore Ministry of Education and the National Natural Science Foundation of China (No. 21233006). We thank Prof. D. Zhao for stimulating discussions and for his assistance of pore size measurement.

Notes and references

[a] Department of Chemistry, National University of Singapore, Singapore.117543; E-mail: chmch@nus.edu.sg.

[b] Sustainable Energy Laboratory, China University of Geoscience, Whuan 430074, China.

Electronic Supplementary Information (ESI) available: [Instrument calibration, FTIR, PXRD, CO_2 and N_2 adsorption isotherms on MTF material and calculated temperature of desorption].

1. K. Sumida, D. L. Rogow, J. A. Mason, T. M. McDonald, E. D. Bloch, Z. R. Herm, T.-H. Bae and J. R. Long, *Chem. Rev.*, 2011, **112**, 724-781.
2. A. Samanta, A. Zhao, G. K. H. Shimizu, P. Sarkar and R. Gupta, *Industrial & Engineering Chemistry Research*, 2011, **51**, 1438-1463.
3. J.-R. Li, Y. Ma, M. C. McCarthy, J. Sculley, J. Yu, H.-K. Jeong, P. B. Balbuena and H.-C. Zhou, *Coord. Chem. Rev.*, 2011, **255**, 1791-1823.
4. E. J. Granite and H. W. Pennline, *Industrial & Engineering Chemistry Research*, 2002, **41**, 5470-5476.
5. C.-H. H. Cheng-Hsiu Yu, Chung-Sung Tan, *Aerosol and Air Quality Research*, 2012, **12**, 745–769.
6. G. T. Rochelle, *Science*, 2009, **325**, 1652-1654.
7. H. Kim, Y. Kim, M. Yoon, S. Lim, S. M. Park, G. Seo and K. Kim, *J. Am. Chem. Soc.*, 2010, **132**, 12200-12202.
8. S. Sircar, T. C. Golden and M. B. Rao, *Carbon*, 1996, **34**, 1-12.
9. A. Phan, C. J. Doonan, F. J. Uribe-Romo, C. B. Knobler, M. O'Keeffe and O. M. Yaghi, *Acc. Chem. Res.*, 2009, **43**, 58-67.
10. Z. Yang, X. Peng and D. Cao, *The Journal of Physical Chemistry C*, 2013.
11. Z. Xiang, D. Cao, W. Wang, W. Yang, B. Han and J. Lu, *The Journal of Physical Chemistry C*, 2012, **116**, 5974-5980.
12. R. Babarao, S. Dai and D.-e. Jiang, *Langmuir*, 2011, **27**, 3451-3460.
13. Y. Lin, Q. Yan, C. Kong and L. Chen, *Sci. Rep.*, 2013, **3**.
14. W. Lu, D. Yuan, J. Sculley, D. Zhao, R. Krishna and H.-C. Zhou, *J. Am. Chem. Soc.*, 2011, **133**, 18126-18129.
15. Z. Xiang, X. Zhou, C. Zhou, S. Zhong, X. He, C. Qin and D. Cao, *J. Mater. Chem.*, 2012, **22**, 22663-22669.
16. R. Dawson, D. J. Adams and A. I. Cooper, *Chemical Science*, 2011, **2**, 1173-1177.
17. Z. Xiang and D. Cao, *Journal of Materials Chemistry A*, 2013, **1**, 2691-2718.
18. A. Demessence, D. M. D'Alessandro, M. L. Foo and J. R. Long, *J. Am. Chem. Soc.*, 2009, **131**, 8784-8786.
19. A. Torrisi, R. G. Bell and C. Mellot-Draznieks, *Crystal Growth & Design*, 2010, **10**, 2839-2841.
20. G. Yang, H. Han, C. Du, Z. Luo and Y. Wang, *Polymer*, 2010, **51**, 6193-6202.
21. M. G. Schwab, B. Fassbender, H. W. Spiess, A. Thomas, X. Feng and K. Müllen, *J. Am. Chem. Soc.*, 2009, **131**, 7216-7217.
22. H. Ma, H. Ren, X. Zou, S. Meng, F. Sun and G. Zhu, *Polymer Chemistry*, 2014, **5**, 144-152.
23. L. Liu, P.-Z. Li, L. Zhu, R. Zou and Y. Zhao, *Polymer*, 2013, **54**, 596-600.
24. P. Parilla, *http://www.hydrogen.energy.gov/pdfs/review12/st014_parilla_2012_o.pdf*, **Hydrogen Sorbent Measurement Qualification and Characterization**
25. A. Hamaed, T. K. A. Hoang, G. Moula, R. Aroca, M. L. Trudeau and D. M. Antonelli, *J. Am. Chem. Soc.*, 2011, **133**, 15434-15443.
26. A. Hamaed, M. Trudeau and D. M. Antonelli, *J. Am. Chem. Soc.*, 2008, **130**, 6992-6999.
27. D. P. M. Broom, P., *J. Alloys Compd.*, 2007, **446–447**, 687-691.
28. M. P. Suh, H. J. Park, T. K. Prasad and D.-W. Lim, *Chem. Rev.*, 2011, **112**, 782-835.
29. J. P. Perdew and Y. Wang, *Physical Review B*, 1992, **45**, 13244-13249.
30. J. Wang, I. Senkovska, M. Oschatz, M. R. Lohe, L. Borchardt, A. Heerwig, Q. Liu and S. Kaskel, *ACS Appl. Mat. Interfaces*, 2013.
31. A. Deryło-Marczewska, J. Goworek, S. Pikus, E. Kobylas and W. Zgrajka, *Langmuir*, 2002, **18**, 7538-7543.
32. G. Coullerez, D. Léonard, S. Lundmark and H. J. Mathieu, *Surf. Interface Anal.*, 2000, **29**, 431-443.
33. P. Pandey, A. P. Katsoulidis, I. Eryazici, Y. Wu, M. G. Kanatzidis and S. T. Nguyen, *Chem. Mater.*, 2010, **22**, 4974-4979.
34. M. G. Schwab, D. Crespy, X. Feng, K. Landfester and K. Müllen, *Macromol. Rapid Commun.*, 2011, **32**, 1798-1803.
35. R. Ströbel, J. Garche, P. T. Moseley, L. Jörissen and G. Wolf, *J. Power Sources*, 2006, **159**, 781-801.
36. J. A. Mason, K. Sumida, Z. R. Herm, R. Krishna and J. R. Long, *Energy Environ. Sci.*, 2011, **4**, 3030-3040.
37. J. Kim, S.-T. Yang, S. B. Choi, J. Sim, J. Kim and W.-S. Ahn, *J. Mater. Chem.*, 2011, **21**, 3070-3076.
38. K. Sumida, S. Horike, S. S. Kaye, Z. R. Herm, W. L. Queen, C. M. Brown, F. Grandjean, G. J. Long, A. Dailly and J. R. Long, *Chemical Science*, 2010, **1**, 184-191.
39. R. Banerjee, H. Furukawa, D. Britt, C. Knobler, M. O'Keeffe and O. M. Yaghi, *J. Am. Chem. Soc.*, 2009, **131**, 3875-3877.
40. B. Wang, A. P. Cote, H. Furukawa, M. O/'Keeffe and O. M. Yaghi, *Nature*, 2008, **453**, 207-211.
41. G. Li, P. Xiao, P. A. Webley, J. Zhang and R. Singh, *Energy Procedia*, 2009, **1**, 1123-1130.
42. S. R. Caskey, A. G. Wong-Foy and A. J. Matzger, *J. Am. Chem. Soc.*, 2008, **130**, 10870-10871.
43. P. D. C. Dietzel, R. E. Johnsen, H. Fjellvag, S. Bordiga, E. Groppo, S. Chavan and R. Blom, *Chem. Commun.*, 2008, 5125-5127.
44. L. Valenzano, B. Civalleri, S. Chavan, G. T. Palomino, C. O. Areán and S. Bordiga, *The Journal of Physical Chemistry C*, 2010, **114**, 11185-11191.
45. M. Dincă, A. Dailly, Y. Liu, C. M. Brown, D. A. Neumann and J. R. Long, *J. Am. Chem. Soc.*, 2006, **128**, 16876-16883.
46. S.-L. Huang and G.-X. Jin, *CrystEngComm*, 2011, **13**, 6013-6016.

Table of Content

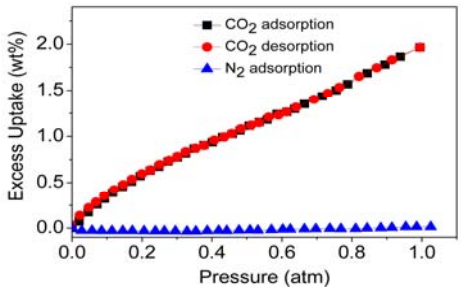

Highly selective CO_2/N_2 adsorption in exposed magnesium metals of a cross-linked organo-magnesium complex.